SEE of Full-Duplex Multi-carrier Bidirectional Wiretap Channels with Multiple Eavesdroppers

Tianyu Yang, Omid Taghizadeh, and Rudolf Mathar
Institute for Theoretical Information Technology, RWTH Aachen University, D-52074 Aachen, Germany
Email: {yang, taghizadeh, mathar}@ti.rwth-aachen.de

***Abstract*—In this work we study the secrecy energy efficiency (SEE) maximization problem for a multi-carrier and multiple-input-multiple-output (MIMO) multiple eavesdroppers communication system. By utilizing the full-duplex (FD) operation, the system is simultaneously capable of bidirectional communication and jamming to the potential eavesdroppers. In particular, we opportunistically utilize different communication and jamming channel conditions at different subcarriers, raised due to multipath fading or large bandwidth, in order to improve the SEE. Due to the non-convex and non-smooth nature of the resulting optimization problem, we propose an iterative solution with a guaranteed convergence to a stationary point based on the successive inner approximation and Dinkelbach's algorithm. The numerical evaluations show a considerable improvement of the system SEE under the condition that the self-interference of the FD transceivers can be efficiently mitigated.**

***Index Terms*—Full-duplex, wiretap channel, secrecy energy efficiency, jamming, multi-carrier, MIMO, multiple eavesdroppers.**

I. Introduction

A Full-duplex (FD) transceiver is capable of transmission and reception at the same time and frequency band, however, suffering from the strong self-interference (SI) from its own transmitter. The recently developed methods for self-interference cancellation (SIC) [1]–[3] have demonstrated practical implementations of FD transceivers in the last few years, and motivated a wide range of related studies. In particular, an FD node can transmit a jamming signal while simultaneously receiving information, thereby improving the information security in the physical layer. It has been shown in [4]–[6], that the application of FD jamming receivers leads to a significantly higher secrecy rate. However, this improvement is obtained at the cost of additional power consumption associated with jamming and SIC. As a result, it is shown in [7] that the application of FD transceivers, although improving the secrecy capacity, result in only a marginal improvement in the secrecy energy efficiency (SEE) in terms of the securely communicated bits-per-Joule, when applied on a single directional communication. Nevertheless, it is observed that the application of FD capability simultaneously on both nodes, enabling bidirectional communication and jamming, lead to a significantly higher SEE. This is mainly grounded in the fact that the jamming from each node, improves the information security at both directions. Hence, the jamming power can be re-used for both communications, enabling an energy-efficient jamming.

Inspired by this, in this work, we extend the SEE-favorable FD bidirectional setup in [7, Section IV] into a scenario with a multi-carrier communication system, supporting a multiple non-collaborative eavesdroppers[1]. In particular, we opportunistically utilize different communication and jamming channel conditions at different subcarriers, raised due to multi-path fading or large bandwidth, in order to improve the SEE. Please note that this is in contrast to the designs [8], [9], only considering HD single antenna transceivers, or the designs [7], [10], [11], only considering the single carrier systems with a single eavesdropper. Due to the non-convex and non-smooth nature of the resulting optimization problem, we propose an iterative solution with guaranteed convergence to a stationary point. This is implemented via a nested combination of the successive inner approximation method [12] and Dinkelbach's algorithm for fractional programs [13]. The numerical results indicate a notable improvement of the system SEE for the proposed system, when SIC is adequately high.

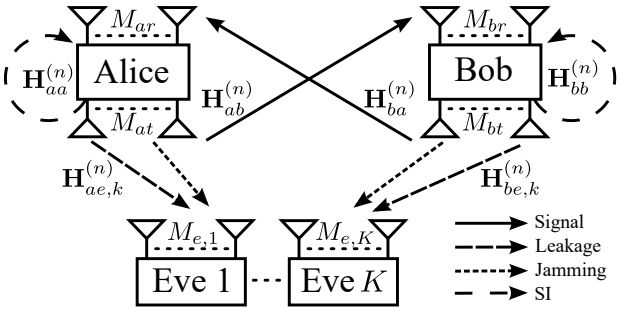

Figure 1. The studied bidirectional multi-carrier MIMO wiretap channel, including FD transceivers Alice, Bob and multiple passive non-collaborative Eves. Upper-index n is the subcarrier index.

A. Mathematical Notation:

In this paper, expectation, trace, inverse, determinant, and Hermitian transpose are denoted by $\mathbb{E}\{\cdot\}$, $\mathrm{tr}(\cdot)$, $(\cdot)^{-1}$, $|\cdot|$ and $(\cdot)^H$, respectively. The Kronecker product is denoted by $\otimes$. $\mathbf{I}_D$ represents the identity matrix with dimension D. $\mathbf{0}_m$ represents an all-zero vector with dimension m. $\perp$ represents the statistical independence. $\mathrm{diag}(\cdot)$ returns a diagonal matrix by putting the off-diagonal elements to zero. The sets of real, non-negative real, complex and the set of all positive semi-definite matrices with Hermitian symmetry are respectively denoted by $\mathbb{R}$, $\mathbb{R}^+$, $\mathbb{C}$ and $\mathcal{H}$. $\{a\}^+$ is equal to a if $a \geq 0$, and zero otherwise. Furthermore, $\mathcal{CN}(\mathbf{x}, \mathbf{X})$ denotes the complex normal distribution with mean $\mathbf{x}$ and covariance $\mathbf{X}$.

II. System Model

We consider a bidirectional wiretap channel with the legitimate transceivers, i.e., Alice and Bob, and K potential illegitimate/undesired receivers, i.e., Eves, see Fig. 1. Moreover, we consider a multi-carrier and MIMO system, where Alice and Bob are capable of FD operation and hence are able to transmit the jamming signal to Eves in order to degrade the decoding capability of Eves while transmit and receive the

[1]Note that the non-colluding scenario subsumes the collaborative eavesdropper scenario as a special case. This is since multiple collaborating eavesdroppers can be equivalently observed as a single multiple antenna eavesdropper

information signal mutually. Alice and Bob are respectively equipped with M_{at} (M_{ar}) and M_{bt} (M_{br}) transmit (receive) antennas. The k-th Eve, where $k \in \mathcal{K}$ and $\mathcal{K}$ is the index set of all Eves, is equipped with $M_{e,k}$ receive antennas. The channel in each subcarrier is assumed to follow a quasi-stationary and flat-fading model. In this regard, channels from Alice to Bob and Bob to Alice, i.e., desired communication channels, are respectively denoted as $\mathbf{H}_{ab}^{(n)} \in \mathbb{C}^{M_{br} \times M_{at}}$ and $\mathbf{H}_{ba}^{(n)} \in \mathbb{C}^{M_{ar} \times M_{bt}}$. Furthermore, channels from Alice to the k-th Eve and Bob to the k-th Eve, i.e., information leakage and jamming channels, are respectively denoted as $\mathbf{H}_{ae,k}^{(n)} \in \mathbb{C}^{M_{e,k} \times M_{at}}$ and $\mathbf{H}_{be,k}^{(n)} \in \mathbb{C}^{M_{e,k} \times M_{bt}}$. Finally, channels from Alice to Alice and Bob to Bob, i.e., SI channels, are respectively denoted as $\mathbf{H}_{aa}^{(n)} \in \mathbb{C}^{M_{ar} \times M_{at}}$ and $\mathbf{H}_{bb}^{(n)} \in \mathbb{C}^{M_{br} \times M_{bt}}$. We have $n \in \mathcal{N}$, where $\mathcal{N}$ is the index set of all subcarriers.

A. Signal model

The transmit signal of n-th subcarrier from Alice and Bob is expressed as

$$\mathbf{u}_{\mathcal{X}}^{(n)} = \underbrace{\mathbf{x}_{\mathcal{X}}^{(n)} + \mathbf{w}_{\mathcal{X}}^{(n)}}_{=:\mathbf{q}_{\text{tx},\mathcal{X}}^{(n)}} + \mathbf{e}_{\text{tx},\mathcal{X}}^{(n)},\ \mathcal{X} \in \{a, b\} \tag{1}$$

where $\{a, b\}$ associates the signal notation to Alice and Bob, and $\mathbf{x}_{\mathcal{X}}^{(n)} \sim \mathcal{CN}\left(\mathbf{0}_{M_{\mathcal{X}t}}, \mathbf{X}_{\mathcal{X}}^{(n)}\right)$ and $\mathbf{w}_{\mathcal{X}}^{(n)} \sim \mathcal{CN}\left(\mathbf{0}_{M_{\mathcal{X}t}}, \mathbf{W}_{\mathcal{X}}^{(n)}\right)$ respectively represent the information and jamming signal of n-th subcarrier. $\mathbf{q}_{\text{tx},\mathcal{X}}^{(n)} \in \mathbb{C}^{M_{\mathcal{X}t}}$ is the intended transmit signal of n-th subcarrier. Moreover, due to the effect of the self-interference in the system with FD transceivers, the distortion signal caused by hardware inaccuracies, e.g., digital-to-analog converter noise, power amplifier noise and oscillator phase noise, become considerable. Thus the impact of transmit chain inaccuracies, i.e., transmit distortion of n-th subcarrier, is denoted as $\mathbf{e}_{\text{tx},\mathcal{X}}^{(n)} \in \mathbb{C}^{M_{\mathcal{X}t}}$, more details are shown in Subsection II-B.

The received signal of n-th subcarrier at Alice and Bob is formulated as

$$\mathbf{y}_{\mathcal{X}}^{(n)} = \underbrace{\mathbf{H}_{\mathcal{Y}\mathcal{X}}^{(n)}\mathbf{u}_{\mathcal{Y}}^{(n)} + \mathbf{H}_{\mathcal{X}\mathcal{X}}^{(n)}\mathbf{u}_{\mathcal{X}}^{(n)} + \mathbf{n}_{\mathcal{X}}^{(n)}}_{=:\mathbf{q}_{\text{rx},\mathcal{X}}^{(n)}} + \mathbf{e}_{\text{rx},\mathcal{X}}^{(n)}, \tag{2}$$

where $\mathcal{X} \neq \mathcal{Y} \in \{a, b\}$, and $\mathbf{n}_{\mathcal{X}}^{(n)} \sim \mathcal{CN}\left(\mathbf{0}_{M_{\mathcal{X}r}}, N_{\mathcal{X}}^{(n)}\mathbf{I}_{M_{\mathcal{X}r}}\right)$ is the additive white noise at n-th subcarrier. Similarly to the transmit side, the receiver distortion of n-th subcarrier, denoted as $\mathbf{e}_{\text{rx},\mathcal{X}}^{(n)} \in \mathbb{C}^{M_{\mathcal{X}r}}$, models the combined impact of receiver chain inaccuracies, e.g., analog-to-digital converter noise, oscillator phase noise and automatic gain control error, see Subsection II-B for more details. Note that the received signal $\mathbf{y}_{\mathcal{X}}^{(n)}$ contains the known self-interference signal $\mathbf{x}_{\mathcal{X}}^{(n)}$ and $\mathbf{w}_{\mathcal{X}}^{(n)}$. Therefore, the recently progressed SIC methods [1]–[3] can be applied to subtract the known, i.e., undistorted, received signal and hence the obtained received signal of n-th subcarrier at Alice and Bob after SIC is written as

$$\begin{aligned}\tilde{\mathbf{y}}_{\mathcal{X}}^{(n)} &= \mathbf{y}_{\mathcal{X}}^{(n)} - \mathbf{H}_{\mathcal{X}\mathcal{X}}^{(n)}\left(\mathbf{x}_{\mathcal{X}}^{(n)} + \mathbf{w}_{\mathcal{X}}^{(n)}\right) \\ &= \mathbf{H}_{\mathcal{Y}\mathcal{X}}^{(n)}\mathbf{u}_{\mathcal{Y}}^{(n)} + \mathbf{H}_{\mathcal{X}\mathcal{X}}^{(n)}\mathbf{e}_{\text{tx},\mathcal{X}}^{(n)} + \mathbf{n}_{X}^{(n)} + \mathbf{e}_{\text{rx},\mathcal{X}}^{(n)} \\ &= \mathbf{H}_{\mathcal{Y}\mathcal{X}}^{(n)}\mathbf{x}_{\mathcal{Y}}^{(n)} + \mathbf{z}_{\mathcal{X}}^{(n)},\end{aligned} \tag{3}$$

where $\mathcal{X} \neq \mathcal{Y} \in \{a, b\}$ and

$$\mathbf{z}_{\mathcal{X}}^{(n)} := \mathbf{H}_{\mathcal{Y}\mathcal{X}}^{(n)}\left(\mathbf{w}_{\mathcal{Y}}^{(n)} + \mathbf{e}_{\text{tx},\mathcal{Y}}^{(n)}\right) + \mathbf{H}_{\mathcal{X}\mathcal{X}}^{(n)}\mathbf{e}_{\text{tx},\mathcal{X}}^{(n)} + \mathbf{n}_{\mathcal{X}}^{(n)} + \mathbf{e}_{\text{rx},\mathcal{X}}^{(n)} \tag{4}$$

is the interference-plus-noise of n-th subcarrier at Alice and Bob.

Similarly, the received signal of n-th subcarrier at k-th Eve is written as

$$\begin{aligned}\mathbf{y}_{\mathcal{X}e,k}^{(n)} &= \mathbf{H}_{ae,k}^{(n)}\mathbf{u}_{a}^{(n)} + \mathbf{H}_{be,k}^{(n)}\mathbf{u}_{b}^{(n)} + \mathbf{n}_{e,k}^{(n)} \\ &= \mathbf{H}_{\mathcal{X}e,k}^{(n)}\mathbf{x}_{\mathcal{X}}^{(n)} + \mathbf{z}_{\mathcal{X}e,k}^{(n)},\end{aligned} \tag{5}$$

where $\mathcal{X} \in \{a, b\}, \mathbf{n}_{e,k}^{(n)} \sim \mathcal{CN}\left(\mathbf{0}_{M_{e,k}}, N_{e}^{(n)}\mathbf{I}_{M_{e,k}}\right)$ is the additive white noise at n-th subcarrier and

$$\begin{aligned}\mathbf{z}_{\mathcal{X}e,k}^{(n)} := \mathbf{H}_{\mathcal{X}e,k}^{(n)}&\left(\mathbf{w}_{\mathcal{X}}^{(n)} + \mathbf{e}_{\text{tx},\mathcal{X}}^{(n)}\right) \\ &+ \mathbf{H}_{\mathcal{Y}e,k}^{(n)}\left(\mathbf{x}_{\mathcal{Y}}^{(n)} + \mathbf{w}_{\mathcal{Y}}^{(n)} + \mathbf{e}_{\text{tx},\mathcal{Y}}^{(n)}\right) + \mathbf{n}_{e,k}^{(n)}\end{aligned} \tag{6}$$

is the interference-plus-noise of n-th subcarrier at k-th Eve. Note that the information signal of non-intended path is considered as an interference for Eve. However, Eve may have the capability to decode it and hence to reduce the received signal from the non-intended information path. We consider and evaluate both scenarios without loss of generality.

B. Residual SI model

As mentioned in Subsection II-A, due to the inaccuracy of the transmit and receiver chains as well as the strong SI channels[2], the impact of distortion signal becomes significant in FD-enabled systems. The impact of inaccuracies in transmit and receiver chains can be modeled by injecting additive Gaussian-distributed and independent distortion terms, see [14, Subsection II.C] and [14, Subsection II.D]. Moreover the collective power of the distortion signals are proportional to the power of intended transmit and receiver signal at the corresponding chains. In our system these are expressed as

$$\mathbf{e}_{\text{tx},\mathcal{X}}^{(n)} \sim \mathcal{CN}\left(\mathbf{0}_{M_{\mathcal{X}t}}, \kappa_{\mathcal{X}}^{(n)}\text{diag}\left(\sum_{n\in\mathcal{N}}\mathbb{E}\left\{\mathbf{q}_{\text{tx},\mathcal{X}}^{(n)}\left(\mathbf{q}_{\text{tx},\mathcal{X}}^{(n)}\right)^{H}\right\}\right)\right), \tag{7}$$

$$\mathbf{e}_{\text{rx},\mathcal{X}}^{(n)} \sim \mathcal{CN}\left(\mathbf{0}_{M_{\mathcal{X}r}}, \beta_{\mathcal{X}}^{(n)}\text{diag}\left(\sum_{n\in\mathcal{N}}\mathbb{E}\left\{\mathbf{q}_{\text{rx},\mathcal{X}}^{(n)}\left(\mathbf{q}_{\text{rx},\mathcal{X}}^{(n)}\right)^{H}\right\}\right)\right), \tag{8}$$

$$\mathbf{e}_{\text{tx},\mathcal{X}}^{(n)} \perp \mathbf{q}_{\text{tx},\mathcal{X}}^{(n)}\ ,\quad \mathbf{e}_{\text{rx},\mathcal{X}}^{(n)} \perp \mathbf{q}_{\text{rx},\mathcal{X}}^{(n)}, \tag{9}$$

where $\mathcal{X} \in \{a, b\}, \kappa_{\mathcal{X}}^{(n)}, \beta_{\mathcal{X}}^{(n)} \in \mathbb{R}^{+}$ represent the transmit and receive distortion coefficients, relating the collective power of the intended transmit and receive signal to the distortion signal variance in the n-th subcarrier[3] [15]. Note that (9) indicates the statistical independence between the distortion signal and the intended transmit/receive signals. For more details on the used distortion model, please see [14], [16], [15, Subsection II.A].

[2]Usually the SI channel is up to 100dB stronger than the communication channels, due to the proximity of the transmit and receiver chains on the same device [14].

[3]The distortion coefficients associated with different subcarriers may be different if, e.g., the subcarrier spacing is not equal over all bands, or the power spectral density of the distortion signals are not completely flat.

$$\boldsymbol{\Sigma}_{\mathcal{X}}^{(n)} = \mathbb{E}\left\{\mathbf{z}_{\mathcal{X}}^{(n)}\left(\mathbf{z}_{\mathcal{X}}^{(n)}\right)^H\right\} = N_{\mathcal{X}}^{(n)}\mathbf{I}_{M_{\mathcal{X}r}} + \mathbf{H}_{\mathcal{Y}\mathcal{X}}^{(n)}\mathbf{W}_{\mathcal{Y}}^{(n)}\left(\mathbf{H}_{\mathcal{Y}\mathcal{X}}^{(n)}\right)^H + \mathbf{H}_{\mathcal{X}\mathcal{X}}^{(n)}\left(\kappa_{\mathcal{X}}^{(n)}\sum_{n\in\mathcal{N}}\text{diag}\left(\mathbf{X}_{\mathcal{X}}^{(n)}+\mathbf{W}_{\mathcal{X}}^{(n)}\right)\right)\left(\mathbf{H}_{\mathcal{X}\mathcal{X}}^{(n)}\right)^H + \beta_{\mathcal{X}}^{(n)}\text{diag}\left(\sum_{n\in\mathcal{N}}\mathbf{H}_{\mathcal{X}\mathcal{X}}^{(n)}\left(\mathbf{X}_{\mathcal{X}}^{(n)}+\mathbf{W}_{\mathcal{X}}^{(n)}\right)\left(\mathbf{H}_{\mathcal{X}\mathcal{X}}^{(n)}\right)^H\right), \tag{15}$$

$$\boldsymbol{\Sigma}_{\mathcal{X}e,k}^{(n)} = \mathbb{E}\left\{\mathbf{z}_{\mathcal{X}e,k}^{(n)}\left(\mathbf{z}_{\mathcal{X}e,k}^{(n)}\right)^H\right\} = N_{e,k}^{(n)}\mathbf{I}_{M_{e,k}} + \mathbf{H}_{\mathcal{X}e,k}^{(n)}\mathbf{W}_{\mathcal{X}}^{(n)}\left(\mathbf{H}_{\mathcal{X}e,k}^{(n)}\right)^H + \mathbf{H}_{\mathcal{Y}e,k}^{(n)}\left(\alpha_{\mathcal{X}e}\mathbf{X}_{\mathcal{Y}}^{(n)}+\mathbf{W}_{\mathcal{Y}}^{(n)}\right)\left(\mathbf{H}_{\mathcal{Y}e,k}^{(n)}\right)^H + \mathbf{H}_{\mathcal{X}e,k}^{(n)}\left(\kappa_{\mathcal{X}}^{(n)}\sum_{n\in\mathcal{N}}\text{diag}\left(\mathbf{X}_{\mathcal{X}}^{(n)}+\mathbf{W}_{\mathcal{X}}^{(n)}\right)\right)\left(\mathbf{H}_{\mathcal{X}e,k}^{(n)}\right)^H + \mathbf{H}_{\mathcal{Y}e,k}^{(n)}\left(\kappa_{\mathcal{Y}}^{(n)}\sum_{n\in\mathcal{N}}\text{diag}\left(\mathbf{X}_{\mathcal{Y}}^{(n)}+\mathbf{W}_{\mathcal{Y}}^{(n)}\right)\right)\left(\mathbf{H}_{\mathcal{Y}e,k}^{(n)}\right)^H, \tag{16}$$

C. Power consumption model

The total consumed power of Alice and Bob are expressed as

$$\begin{aligned} P_{\mathcal{X}} &= \tilde{P}_{\mathcal{X}} + P_{\mathcal{X},0} + P_{\text{FD}} \\ &= \frac{1}{\mu_{\mathcal{X}}}\sum_{n\in\mathcal{N}}\mathbb{E}\left\{\|\mathbf{u}_{\mathcal{X}}^{(n)}\|_2^2\right\} + P_{\mathcal{X},0} + P_{\text{FD}} \\ &= \frac{1+\sum_{n\in\mathcal{N}}\kappa_{\mathcal{X}}^{(n)}}{\mu_{\mathcal{X}}}\sum_{n\in\mathcal{N}}\text{tr}\left(\mathbf{X}_{\mathcal{X}}^{(n)}+\mathbf{W}_{\mathcal{X}}^{(n)}\right) + P_{\mathcal{X},0} + P_{\text{FD}}, \end{aligned} \tag{10}$$

where $\mathcal{X} \in \{a,b\}, \tilde{P}_{\mathcal{X}}, P_{\mathcal{X},0}$ and $\mu_{\mathcal{X}}$ respectively represent the power consumption for transmission, zero-state power and power amplifier efficiency. Moreover, P_{FD} denotes the power consumption for the implementation of SIC function. Then, the total power consumption of the system is written as

$$P_{\text{tot}} = P_a + P_b. \tag{11}$$

D. Secrecy energy efficiency

The secrecy rate of defined bidirectional system for the k-th eavesdropper in n-th subcarrier is written as

$$\begin{aligned} \mathcal{I}_k^{(n)} &= \Big\{\underbrace{\mathcal{I}_{ab}^{(n)} - \mathcal{I}_{ae,k}^{(n)}}_{=:\mathcal{C}_{ab,k}^{(n)}}\Big\}^+ + \Big\{\underbrace{\mathcal{I}_{ba}^{(n)} - \mathcal{I}_{be,k}^{(n)}}_{=:\mathcal{C}_{ba,k}^{(n)}}\Big\}^+ \\ &= \left\{\log_2\left|\mathbf{I}+\mathbf{Q}_{ab}^{(n)}\left(\boldsymbol{\Sigma}_b^{(n)}\right)^{-1}\right| - \log_2\left|\mathbf{I}+\mathbf{Q}_{ae,k}^{(n)}\left(\boldsymbol{\Sigma}_{ae,k}^{(n)}\right)^{-1}\right|\right\}^+ \\ &+ \left\{\log_2\left|\mathbf{I}+\mathbf{Q}_{ba}^{(n)}\left(\boldsymbol{\Sigma}_a^{(n)}\right)^{-1}\right| - \log_2\left|\mathbf{I}+\mathbf{Q}_{be,k}^{(n)}\left(\boldsymbol{\Sigma}_{be,k}^{(n)}\right)^{-1}\right|\right\}^+, \end{aligned} \tag{12}$$

where $\mathcal{I}_{ab}^{(n)}(\mathcal{I}_{ba}^{(n)})$ represents the information capacity of Alice to Bob (Bob to Alice) path in n-th subcarrier. Similarly, $\mathcal{I}_{ae,k}^{(n)}(\mathcal{I}_{be,k}^{(n)})$ represents the information capacity of Alice (Bob) to k-th Eve path in n-th subcarrier. Moreover, $\mathbf{Q}_{\mathcal{X}\mathcal{Y}}^{(n)}$, $\mathbf{Q}_{\mathcal{X}e,k}^{(n)}$, $\boldsymbol{\Sigma}_{\mathcal{X}}^{(n)}$ and $\boldsymbol{\Sigma}_{\mathcal{X}e,k}^{(n)}$ with $\mathcal{X}\neq\mathcal{Y}\in\{a,b\}$, given in (13), (14), (15) and (16), represent the covariance of the signal terms and the interference-plus-noise terms of the n-th subcarrier at Alice, Bob and k-th Eve.

$$\mathbf{Q}_{\mathcal{X}\mathcal{Y}}^{(n)} = \mathbf{H}_{\mathcal{X}\mathcal{Y}}^{(n)}\mathbf{X}_{\mathcal{X}}^{(n)}\left(\mathbf{H}_{\mathcal{X}\mathcal{Y}}^{(n)}\right)^H \tag{13}$$

$$\mathbf{Q}_{\mathcal{X}e,k}^{(n)} = \mathbf{H}_{\mathcal{X}e,k}^{(n)}\mathbf{X}_{\mathcal{X}}^{(n)}\left(\mathbf{H}_{\mathcal{X}e,k}^{(n)}\right)^H \tag{14}$$

Note that in (16) the coefficient α_{ae} and α_{be} represent the ratio of decoding capability at Eve for non-intended information path. Specifically, if $\alpha_{ae}=\alpha_{be}=1$ we consider that Eves treat the information signal of non-intended path as noise. Conversely, if $\alpha_{ae}=\alpha_{be}=0$ we consider that Eves could decode the information signal of non-intended path. The system performance related to these two scenarios is numerically analyzed in Section IV.

Following [17], the achievable secrecy rate of defined multiple non-colluding eavesdroppers system is expressed as[4]

$$R_s = \min_{k\in\mathcal{K}}\sum_{n\in\mathcal{N}}\mathcal{I}_k^{(n)}. \tag{17}$$

Then, the secrecy energy efficiency is consequently written as

$$\text{SEE} = \frac{R_s}{P_{\text{tot}}}. \tag{18}$$

E. Remarks

In this work, we assume the availability of CSI on all channels. This is achievable for Alice-Eve and Bob-Eve channels when Eve is a collaborative node, e.g., an untrusted but collaborative communication node [18]. Additionally, the study with perfect CSI provides a valuable performance bound of the system, also when the instantaneous CSI is not available.

III. SEE Maximization

In this part we intend to enhance the defined SEE in (18). The optimization problem of the system is written as

$$\max_{\mathbb{X},\mathbb{W}} \quad \text{SEE} \tag{19a}$$

$$\text{s.t.} \quad \tilde{P}_a \le P_{a,\max}, \tag{19b}$$

$$\tilde{P}_b \le P_{b,\max}, \tag{19c}$$

where $\mathbb{X}$ and $\mathbb{W}$ represent the set of $\mathbf{X}_{\mathcal{X}}^{(n)}\in\mathcal{H}$ and $\mathbf{W}_{\mathcal{X}}^{(n)}\in\mathcal{H}$, $\forall n\in\mathcal{N}$, $\mathcal{X}\in\{a,b\}$ and $P_{a,\max}, P_{b,\max}\in\mathbb{R}^+$ represent the maximum total transmission power for Alice and Bob.

Note that due to the operation $\{\cdot\}^+$ and the expression form of minimum value in (17), the problem in (19) is intractable. Nevertheless, with the utilization of the following lemma the non-linear operation $\{\cdot\}^+$ can be removed during the optimization. Then, by introducing auxiliary variables the problem in (19) can be transformed into a more tractable form.

Lemma III.1. *Let $\mathbf{X}_a^{(n)\star}$ and $\mathbf{X}_b^{(n)\star}$ be the optimal solution at the optimality. The operator $\{\cdot\}^+$ has no influence at the optimality of (19), since $\mathbf{X}_a^{(n)\star}$ and $\mathbf{X}_b^{(n)\star}$ lead to non-negative $\mathcal{C}_{ab,k}^{(n)}$ and $\mathcal{C}_{ba,k}^{(n)}$.*

Proof. Assume at the optimality the operator $\{\cdot\}^+$ has impact on n-th subcarrier, i.e., at least one of $\mathcal{C}_{ab,k}^{(n)}$ and $\mathcal{C}_{ba,k}^{(n)}, \forall k\in\mathcal{K}$, is negative, a better value of $\mathbf{X}_a^{(n)}=\mathbf{0}$ and/or $\mathbf{X}_b^{(n)}=\mathbf{0}$ could

[4]Note that this non-colluding scenario is a more general case since when $K=1$ the system model degrades to an equivalent multiple colluding eavesdroppers scenario.

$$T_{\mathcal{XY}}^{[j,l]} \geq \sum_{n\in\mathcal{N}} \left(\log\left|\mathbf{Q}_{\mathcal{X}e}^{(n),[0,l]} + \mathbf{\Sigma}_{\mathcal{X}e,k}^{(n),[0,l]}\right| - \mathrm{tr}\left(\left(\mathbf{Q}_{\mathcal{X}e}^{(n),[0,l]} + \mathbf{\Sigma}_{\mathcal{X}e,k}^{(n),[0,l]}\right)^{-1} \left(\mathbf{Q}_{\mathcal{X}e}^{(n),[0,l]} + \mathbf{\Sigma}_{\mathcal{X}e,k}^{(n),[0,l]} - \mathbf{Q}_{\mathcal{X}e}^{(n),[j,l]} - \mathbf{\Sigma}_{\mathcal{X}e,k}^{(n),[j,l]}\right)\right) - \log\left|\mathbf{\Sigma}_{\mathcal{X}e,k}^{(n)}\right| \right), \quad \forall \mathcal{X}\neq\mathcal{Y}\in\{a,b\},\ \forall k\in\mathcal{K} \tag{24}$$

$$\tilde{\mathcal{I}}_T^{[j,l]} = \sum_{\mathcal{X}\neq\mathcal{Y}\in\{a,b\}} \left(\sum_{n\in\mathcal{N}} \left(\log\left|\mathbf{Q}_{\mathcal{XY}}^{(n)} + \mathbf{\Sigma}_{\mathcal{Y}}^{(n)}\right| - \log\left|\mathbf{\Sigma}_{\mathcal{Y}}^{(n),[0,l]}\right| + \mathrm{tr}\left(\left(\mathbf{\Sigma}_{\mathcal{Y}}^{(n),[0,l]}\right)^{-1} \left(\mathbf{\Sigma}_{\mathcal{Y}}^{(n),[0,l]} - \mathbf{\Sigma}_{\mathcal{Y}}^{(n),[j,l]}\right)\right)\right) - T_{\mathcal{XY}}^{[j,l]} \right) \tag{25}$$

$$\tilde{P}_{\text{tot}}^{[j,l]} = \sum_{\mathcal{X}\in\{a,b\}} \left(\frac{1+\sum_{n\in\mathcal{N}} \kappa_{\mathcal{X}}^{(n)}}{\mu_{\mathcal{X}}} \sum_{n\in\mathcal{N}} \mathrm{tr}\left(\mathbf{X}_{\mathcal{X}}^{(n),[j,l]} + \mathbf{W}_{\mathcal{X}}^{(n),[j,l]}\right) + P_{\mathcal{X},0} \right) + 2P_{\text{FD}} \tag{26}$$

be chosen and the correspondingly reduced power could be applied to other subcarriers with positive $\mathcal{I}_k^{(n)}$. This improves the SEE, which contradicts the optimality assumption. □

By removing the $\{\cdot\}^+$ operation and introducing two auxiliary variables T_{ab} and $T_{ba} \in \mathbb{R}$, the problem (19) can be reformulated as

$$\max_{\substack{\mathbb{X},\mathbb{W},\\ T_{ab},T_{ba}}} \quad \frac{\mathcal{I}_T}{P_{\text{tot}}} \tag{20a}$$

$$\text{s.t.} \quad \tilde{P}_{\mathcal{X}} \leq P_{\mathcal{X},\max}, \quad \forall \mathcal{X}\neq\mathcal{Y}\in\{a,b\}, \tag{20b}$$

$$T_{\mathcal{XY}} \geq \sum_{n\in\mathcal{N}} \left(\log\left|\mathbf{Q}_{\mathcal{X}e}^{(n)} + \mathbf{\Sigma}_{\mathcal{X}e,k}^{(n)}\right| - \log\left|\mathbf{\Sigma}_{\mathcal{X}e,k}^{(n)}\right| \right), \quad \forall \mathcal{X}\neq\mathcal{Y}\in\{a,b\},\ \forall k\in\mathcal{K}, \tag{20c}$$

where $\mathcal{I}_T$ is written as

$$\mathcal{I}_T = \sum_{\substack{\mathcal{X}\neq\mathcal{Y}\\ \in\{a,b\}}} \left(\sum_{n\in\mathcal{N}} \left(\log\left|\mathbf{Q}_{\mathcal{XY}}^{(n)} + \mathbf{\Sigma}_{\mathcal{Y}}^{(n)}\right| - \log\left|\mathbf{\Sigma}_{\mathcal{Y}}^{(n)}\right| \right) - T_{\mathcal{XY}} \right). \tag{21}$$

Note that the problem (20) is still intractable due to the non-concave terms $-\log|\cdot|$ in the objective function (21), the non-convex terms $\log|\cdot|$ in the constrain (20c) and the fractional structure of objective function. To solve the problem we propose an iterative algorithm with nested loops following a successive inner approximation (SIA) method [12] and Dinkelbach's algorithm [13].

A. Iterative SIA based algorithm

The proposed iterative algorithm has a structure of two nested loops. In the outer loops, the intractable terms are approximately substituted with the tractable affine terms. Then, the lower bound based on the approximation is iteratively maximized in the inner loops.

Specifically, in the l-th outer loop the first-order Taylor approximation

$$\log|\mathbf{A}| \leq \log|\mathbf{B}| - \mathrm{tr}\left(\mathbf{B}^{-1}(\mathbf{B}-\mathbf{A})\right) \tag{22}$$

is applied to the intractable terms at the point $\mathbf{B}$. Then, in the j-th inner loop the obtained concave-over-affine fractional structure is resolved via Dinkelbach's algorithm [13] so that the lower bound obtained from the approximation is iteratively improved. Concretely, the variable set $\mathbb{Z} := \{\mathbb{X}, \mathbb{W}\}$ is updated by solving the following optimization

$$\max_{\mathbb{Z}^{[j,l]},T_{ab}^{[j,l]},T_{ba}^{[j,l]}} \quad \tilde{\text{SEE}}^{[j,l]} \tag{23a}$$

$$\text{s.t.} \quad (20b), (24), \tag{23b}$$

where $\tilde{\text{SEE}}^{[j,l]} = \tilde{\mathcal{I}}_T^{[j,l]} - \lambda^{[j,l]}\tilde{P}_{\text{tot}}^{[j,l]}$, $\tilde{\mathcal{I}}_T^{[j,l]}$ and $\tilde{P}_{\text{tot}}^{[j,l]}$ are given in (25) and (26) respectively. Moreover, λ is an auxiliary variable and $\mathbf{Q}_{\mathcal{XY}}^{(n),[j,l]}, \mathbf{Q}_{\mathcal{X}e}^{(n),[j,l]}, \mathbf{\Sigma}_{\mathcal{X}}^{(n),[j,l]}, \mathbf{\Sigma}_{\mathcal{X}e,k}^{(n),[j,l]}, \mathcal{X}\neq\mathcal{Y}\in\{a,b\}$ are calculated from (13), (14), (15), (16) at the j-th inner loop and l-th outer loop.

Note that with a fixed $\lambda^{[j,l]}$ the optimization in (23) is a jointly convex problem over $\mathbb{Z}^{[j,l]}, T_{ab}^{[j,l]}, T_{ba}^{[j,l]}$. It can be efficiently implemented via MAX-DET algorithm [19] and solved via advanced convex optimization solvers. Then, according to Dinkelbach's algorithm the variable $\lambda^{[j,l]}$ is updated as

$$\lambda^{[j,l]} = \frac{\tilde{\mathcal{I}}_T^{[j,l]}}{\tilde{P}_{\text{tot}}^{[j,l]}}. \tag{27}$$

The full iterative SIA based algorithm with inner and outer loops is shown in Algorithm 1.

B. Convergence

We firstly analyze the convergence of the inner loop. According to the proof in [20, Proposition 3.2] the applied Dinkelbach's algorithm for our concave-over-affine fractional structure converges to a global optimum point in each inner loop. This global optimum point also leads to the convergence in the outer loop because of the monotonic improvement and the fact that SEE is bounded from above. Please note that the bound obtained via the utilization of (22) is a tight and global bound. Additionally, the slope at the approximation point remains the same as the original function. Thus the outer loop converges to a stationary point according to [12, Theorem 1]. The convergence behaviour is numerically studied in Subsection IV-A.

Algorithm 1 Iterative SIA based algorithm for SEE maximization. ε_F (ε_{SEE}) denotes the convergence threshold for the inner (outer) iterations.

```
j, l ← 0;   set iteration number to zero
λ^[0,0] ← 0;   Initialize to zero according to Dinkelbach's algorithm
ℤ^[0,0] ← 0;   initialize to zero matrices
repeat
    l ← l + 1;
    λ^[0,l] ← λ^[j,l−1]; ℤ^[0,l] ← ℤ^[j,l−1]; j ← 0;
    repeat
        j ← j + 1;
        ℤ^[j,l], T_ab^[j,l], T_ba^[j,l] ← solve (23);
        F ← S̃ẼE^[j,l] (ℤ^[j,l], ℤ^[0,l], λ^[j,l]);
        λ^[j,l] ← (27);
    until F ≤ ε_F
until λ^[j,l] − λ^[0,l] ≤ ε_SEE
return {ℤ^[j,l], λ^[j,l]}
```

IV. Simulation Results

In this section the studied bidirectional wiretap channel with multiple eavesdrops is numerically evaluated in terms

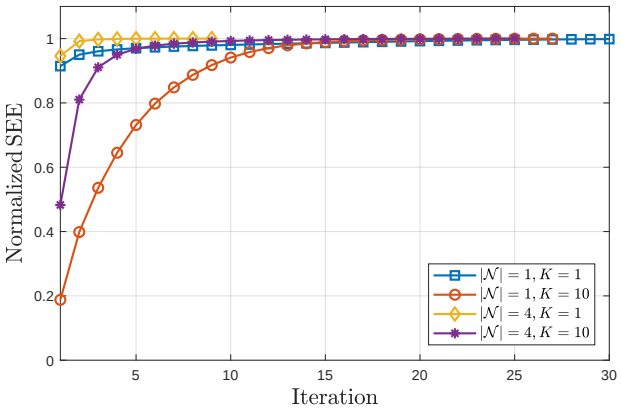

Figure 2. Convergence behavior of the proposed iterative method.

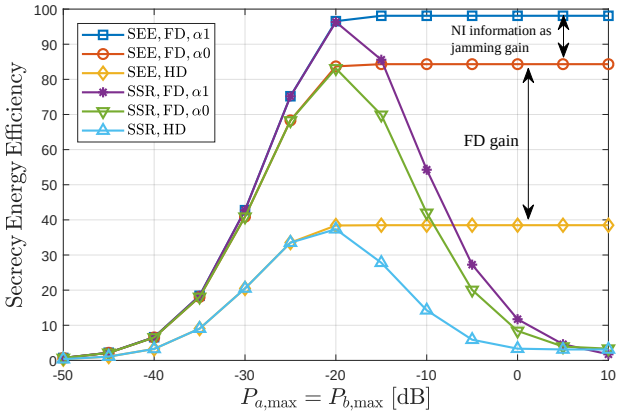

Figure 3. Impact of maximum transmit power per node.

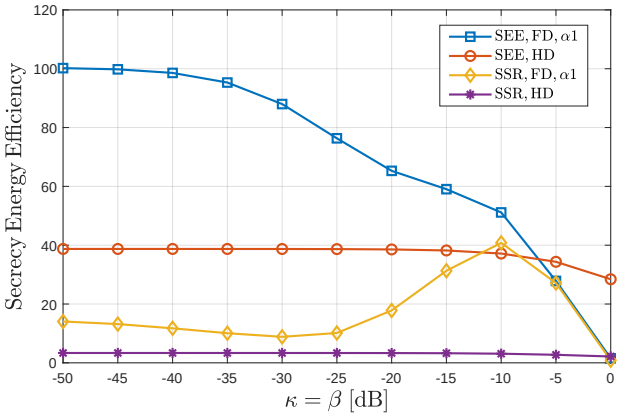

Figure 4. Impact of transceiver dynamic range.

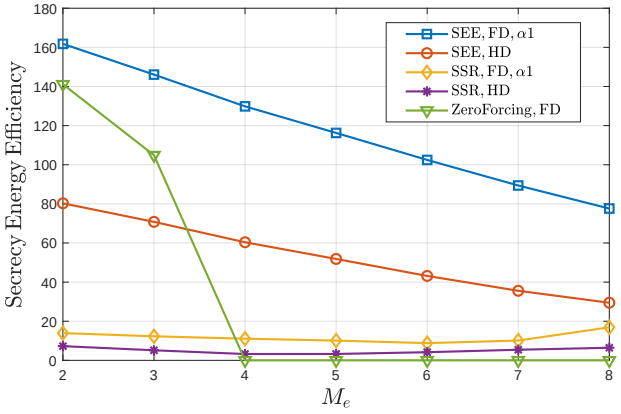

Figure 5. Impact of Eve's antenna number.

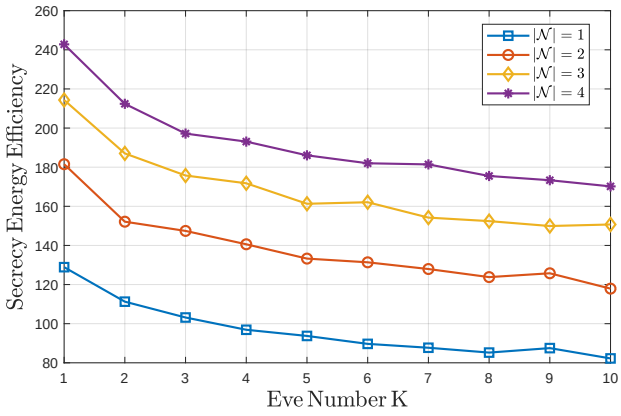

Figure 6. Impact of number of Eves and subcarriers.

of secrecy energy efficiency. We mainly compare the FD-enabled system to the system with all HD nodes. Moreover, the proposed SEE-specific design is also evaluated in comparison to the system design targeting the maximization of sum secrecy capacity without the energy efficiency concern. We assume that the channels $\mathbf{H}_{\mathcal{X}}^{(n)}$ are following an uncorrelated Rayleigh flat-fading distribution, with variance $\eta_{\mathcal{X}} = \bar{\eta}/d_{\mathcal{X}}^2$ for each element, where $\mathcal{X} \in \{ab, ba, ae, be\}$ and $d_{\mathcal{X}}$ is the link distance. Furthermore, following [21] for the SI channels we have $\mathbf{H}_{\mathcal{X}\mathcal{X}}^{(n)} \sim \mathcal{CN}\left(\sqrt{\frac{\rho_{\text{si}} K_R}{1+K_R}}\mathbf{H}_0, \frac{\rho_{\text{si}}}{1+K_R}\mathbf{I}_{M_{\mathcal{X}r}} \otimes \mathbf{I}_{M_{\mathcal{X}t}}\right)$, where $\mathcal{X} \in \{a, b\}$, ρ_{si} represents the SI channel strength, $\mathbf{H}_0$ is a matrix with all elements equal to 1 and K_R is the Rician coefficient. The resulting system performance is averaged over 200 channel realizations. Unless otherwise is stated the default values of simulation parameters are as following: $M := M_{\mathcal{X}t} = M_{\mathcal{X}r} = M_e = 4$, $P_{\max} := P_{\mathcal{X},\max} = 0$dB, $P_0 := P_{\mathcal{X},0} = -20$dB, $\mu := \mu_{\mathcal{X}} = 0.9$, $\kappa := \kappa_{\mathcal{X}}^{(n)} = \beta_{\mathcal{X}}^{(n)} = -40$dB, $N := N_{\mathcal{X}}^{(n)} = N_e^{(n)} = -40$dB, $\alpha := \alpha_{\mathcal{X}e} = 1$, $\mathcal{X} \in \{a, b\}$. Moreover, we set $|\mathcal{N}| = 1$, $K = |\mathcal{K}| = 4$, $K_R = 10$, $\rho_{\text{si}} = 0$dB, $P_{\text{FD}} = 0$, $\bar{\eta} = -20$dB. We consider a equidistant geometry setup where the distances between Alice and Bob and between any eavesdropper and Alice or Bob are equal to one.

A. Algorithm convergence

As the proposed algorithm is an iterative solution, we firstly present the convergence behavior. In Fig. 2 the convergence behavior is depicted for the setups with different eavesdropper number K and subcarrier number $|\mathcal{N}|$. The curves show the resulting normalized SEE after each iteration of the outer loop. It is observed that the proposed algorithm has a monotonic improvement and converges in 10-30 iterations. It is also shown that the results after the first iteration of the setups with various K and $|\mathcal{N}|$ have notable difference. Specifically, the setups with larger number of Eves have bad performance at the beginning of iterations and thus need more iterations to converge. Conversely, the setups with larger number of subcarriers can achieve a good performance already at the first few iterations, which needs less iterations to converge.

B. Performance comparison

In this part the performance of the proposed bidirectional wiretap system is evaluated in terms of SEE. In general we compare the proposed FD bidirectional system with the target of SEE maximization to the following systems: HD bidirectional system with the target of SEE maximization; FD

(HD) bidirectional system with the target of sum secrecy rate (SSR) maximization. In the figures, these four systems are denoted as 'SEE,FD', 'SEE,HD', 'SSR,FD' and 'SSR,HD', respectively. The HD bidirectional communication is facilitated via time-division-duplex (TDD) scheme. Moreover, regarding to the decoding capability of Eve, we have two scenarios where Eve could (could not) decode the non-intended (NI) information path, i.e., $\alpha = 0$ ($\alpha = 1$), denoted as 'α0' ('α1') in the figures.

1) Total power constrains: In Fig. 3 the resulting SEE related to total allowed transmit power of each node is depicted. It is observed that under low power constrains ($P_{\max}$ lower than -20dB) the resulting SEE of all systems increases with the power. Nevertheless, under high power constrains, the performance of secrecy energy efficiency concerned systems saturates while the performance of secrecy rate concerned systems decreases dramatically. Moreover, a significant gain of FD systems is observed compared to the HD systems, which is benefiting from the reused jamming in both directions. Furthermore, starting from -30dB of $P_{\max}$ the impact of the decoding capability of Eve is getting considerable. It is observed that if Eve could not decode the non-intended information signal, a notable gain is obtained.

2) Transceiver accuracy: In Fig. 4 the impact of the transceiver dynamic range is depicted. It is observed that with high transceiver accuracy, i.e., low κ and β, the proposed FD-enabled system shows a significant gain in terms of SEE. However, with increasing κ and β, the performance of the proposed FD-enabled system decreases due to the strong residual SI. With a very bad transceiver accuracy, e.g., $\kappa = \beta = 0$dB, the performance of the FD systems is even much worse than the HD systems.

3) Antenna number of eavesdropper: In Fig. 5 the impact of Eve's antenna number is depicted. In this scenario we study a system with only one eavesdropper. In this regard, if $M_{\mathcal{X}t} > \sum_{k\in\mathcal{K}} M_{e,k}, \forall \mathcal{X} \in \{a, b\}$, it is able to apply zero-forcing to Eve by adding $\text{tr}(\mathbf{Q}_{\mathcal{X}e}) = 0, \forall \mathcal{X} \in \{a, b\}$ in the constrains. Note that this zero-forcing scheme does not require jamming and hence incurs a lower computational complexity. Thus, we also compared our proposed system to this zero-forcing scheme which is denoted as 'Zero Forcing' in Fig. 5. It is observed that with a increasing M_e the resulting SEE of proposed system decrease roughly linearly as expected. Inside the feasible range of M_e for zero-forcing ($M_e < M_{at} = M_{bt} = 4$), the resulting SEE of the proposed system is still better than the result of zero-forcing scheme.

4) Number of Eves and subcarriers: In Fig. 6 the impact of the number of eavesdroppers and subcarriers is depicted. The shown four results are from the proposed FD system with different number of subcarriers. It is observed that the resulting SEE decreases slightly with the increment of K. On the other hand, a larger number of subcarriers can enhance the performance significantly through a large range of Eve's number.

V. Conclusion

In this work we addressed a secrecy energy efficiency maximization problem in an FD-enabled multi-carrier bidirectional wiretap channel with multiple non-collaborative eavesdroppers. We proposed an iterative solution based on the successive inner approximation and Dinkelbach's algorithm. The numerical results show that the proposed system keeps a better performance in terms of secrecy energy efficiency compared to the systems with target of secrecy rate maximization. The results also indicate a significant gain of the FD-enabled bidirectional system compared to the HD system under a high SIC level, due to the reused jamming power. Furthermore, a larger number of subcarriers can also enhance the performance dramatically even with a large number of eavesdroppers.

References

[1] D. Bharadia and S. Katti, "Full duplex MIMO radios," in *11th USENIX Symposium on Networked Systems Design and Implementation (NSDI 14)*. Seattle, WA: USENIX Association, 2014, pp. 359–372.

[2] Y. Hua, P. Liang, Y. Ma, A. C. Cirik, and Q. Gao, "A method for broadband full-duplex mimo radio," *IEEE Signal Processing Letters*, vol. 19, no. 12, pp. 793–796, Dec 2012.

[3] D. Bharadia, E. McMilin, and S. Katti, "Full duplex radios," in *Proceedings of the ACM SIGCOMM 2013 Conference on SIGCOMM*, ser. SIGCOMM '13. New York, NY, USA: ACM, 2013, pp. 375–386.

[4] L. Li, Z. Chen, D. Zhang, and J. Fang, "A full-duplex bob in the MIMO gaussian wiretap channel: Scheme and performance," *IEEE Signal Processing Letters*, vol. 23, no. 1, pp. 107–111, Jan 2016.

[5] F. Zhu, F. Gao, M. Yao, and H. Zou, "Joint information- and jamming-beamforming for physical layer security with full duplex base station," *IEEE Transactions on Signal Processing*, vol. 62, no. 24, pp. 6391–6401, Dec 2014.

[6] Y. Zhou, Z. Z. Xiang, Y. Zhu, and Z. Xue, "Application of full-duplex wireless technique into secure MIMO communication: Achievable secrecy rate based optimization," *IEEE Signal Processing Letters*, vol. 21, no. 7, pp. 804–808, July 2014.

[7] O. Taghizadeh, P. Neuhaus, and R. Mathar, "Can full-duplex jamming reduce the energy-cost of a secure bit?" in *Wireless Communications and Networking Conference (WCNC), 2018 IEEE*. IEEE, 2018, pp. 1–6.

[8] X. Chen and L. Lei, "Energy-efficient optimization for physical layer security in multi-antenna downlink networks with qos guarantee," *IEEE Communications Letters*, vol. 17, no. 4, pp. 637–640, 2013.

[9] D. W. K. Ng, E. S. Lo, and R. Schober, "Energy-efficient resource allocation for secure ofdma systems," *IEEE Transactions on Vehicular Technology*, vol. 61, no. 6, pp. 2572–2585, 2012.

[10] B. Fang, Z. Qian, W. Zhong, and W. Shao, "Energy-efficient secrecy precoding for general mimome wiretap channels," in *Wireless Communications & Signal Processing (WCSP), 2015 International Conference on*. IEEE, 2015, pp. 1–5.

[11] A. Zappone, P.-H. Lin, and E. A. Jorswieck, "Secrecy and energy efficiency in mimo-me systems," in *Signal Processing Advances in Wireless Communications (SPAWC), 2015 IEEE 16th International Workshop on*. IEEE, 2015, pp. 380–384.

[12] B. R. Marks and G. P. Wright, "A general inner approximation algorithm for nonconvex mathematical programs," *Operations research*, vol. 26, no. 4, pp. 681–683, 1978.

[13] W. Dinkelbach, "On nonlinear fractional programming," *Management science*, vol. 13, no. 7, pp. 492–498, 1967.

[14] B. P. Day, A. R. Margetts, D. W. Bliss, and P. Schniter, "Full-duplex bidirectional MIMO: Achievable rates under limited dynamic range," *IEEE Transactions on Signal Processing*, vol. 60, no. 7, pp. 3702–3713, July 2012.

[15] O. Taghizadeh, V. Radhakrishnan, A. C. Cirik, R. Mathar, and L. Lampe, "Hardware impairments aware transceiver design for bidirectional full-duplex MIMO OFDM systems," *IEEE Transactions on Vehicular Technology*, pp. 1–1, 2018.

[16] X. Xia, D. Zhang, K. Xu, W. Ma, and Y. Xu, "Hardware impairments aware transceiver for full-duplex massive MIMO relaying," *IEEE Transactions on Signal Processing*, vol. 63, no. 24, pp. 6565–6580, 2015.

[17] Y. Liang, G. Kramer, H. V. Poor, and S. Shamai, "Compound wiretap channels," *EURASIP Journal on Wireless Communications and Networking*, vol. 2009, p. 5, 2009.

[18] R. Zhang, L. Song, Z. Han, and B. Jiao, "Physical layer security for two-way untrusted relaying with friendly jammers," *IEEE Transactions on Vehicular Technology*, vol. 61, no. 8, pp. 3693–3704, Oct 2012.

[19] L. Vandenberghe, S. Boyd, and S.-P. Wu, "Determinant maximization with linear matrix inequality constraints," *SIAM J. Matrix Anal. Appl.*, vol. 19, no. 2, pp. 499–533, Apr. 1998.

[20] A. Zappone, E. Jorswieck *et al.*, "Energy efficiency in wireless networks via fractional programming theory," *Foundations and Trends® in Communications and Information Theory*, vol. 11, no. 3-4, pp. 185–396, 2015.

[21] M. Duarte, C. Dick, and A. Sabharwal, "Experiment-driven characterization of full-duplex wireless systems," *IEEE Transactions on Wireless Communications*, vol. 11, no. 12, pp. 4296–4307, December 2012.